A novel data processing algorithm in thermal property measurement and defect detection by using one-sided active infrared thermography

V.P. Vavilov*,**[1], V.V. Shiryaev*, A.O. Chulkov*
* Tomsk Polytechnic University, 634028, Tomsk, Savinykh St., 7, Russia
** Tomsk State University, 634050, Tomsk, Lenin Av., 36, Russia

ABSTRACT

The proposed algorithm is based on the analysis of an artificial front-surface pixel-based function which includes temperature and time. This function experiences certain extremums, and the corresponding times can be used for determining thermal diffusivity by the formula similar to the known Parker expression. In thermal NDT, such approach being applied to defect areas, provides diffusivity variations which can be used for the evaluation of defect severity in a particular specimen. In this study, both the theoretical basis and the some experimental implementations of the proposed data processing algorithm have been explored to illustrate its validity in thermal properties measurement and thermal NDT, including thermal tomography.

Keywords: thermal nondestructive testing, modeling, diffusivity measurement, data processing

1. INTRODUCTION

Comparison between one- and two-sided test procedures is an ongoing issue in thermal nondestructive testing (NDT). From the theoretical point of view, a two-sided procedure seems to be the most appropriate to provide a more accurate measurement of thermal properties, as well as a more reliable detection of defects arbitrarily located across a test sample. A good illustration to this statement is the known Parker method intended for determining thermal diffusivity [1]. Basically, this is a two-sided pulsed technique which takes into account material properties averaged by sample thickness. The same statement adheres to thermal NDT of hidden defects. The difficulty in using a one-sided procedure is that it does not provide evident specific points in the front-surface temperature evolution which can be used for reliable data inversion. In practice, another drawback of one-sided procedures is the presence of reflected radiation produced by a heat source used for stimulating test samples.

2. BASIC ANALYSIS

The basic model to be analyzed is a 'classical' plate-like sample (Fig. 1a) stimulated with a heat flux which ensures the power density of Q and operates during the time τ_h (heat pulse duration). The temperature responses on both front (*F*) and rear (*R*) surface of the sample are analyzed at a characteristic heat transit time τ^*. If $\tau^* >> \tau_h$, the heating can be considered as Dirac-like, or flash. The sample contains a void-like defect at the depth l having a lateral size $S_{x,y}$ and thickness d. Both the *F*- and R-surface of the sample experience convective heat exchange characterized by the coefficient h. If hL/K <0.1, where L is the sample thickness and hL/K is the thermal conductivity.

In the adiabatic case, the temperature on the plate rear surface as a function of time is calculated by using the well-known analytical solution for an infinite plate uniformly heated on the front surface by a Dirac pulse:

$$T = \frac{Wa}{KL}\left(1 + 2\sum_{n=1}^{\infty}(-1)^n e^{-n^2\pi^2 Fo}\right), \quad (1)$$

[1] vavilov@tpu.ru; phone 7 913 821-9749; fax 7 382 241-7281

Thermosense: Thermal Infrared Applications XXXVII, edited by Sheng-Jen (Tony) Hsieh, Joseph N. Zalameda,
Proc. of SPIE Vol. 9485, 94850V · © 2015 SPIE · CCC code: 0277-786X/15/$18 · doi: 10.1117/12.2175645

where W is the Dirac pulse energy (in real cases $W = Q\tau_h$), $Fo = a\tau / L^2$ is the Fourier number, and a is the thermal diffusivity.

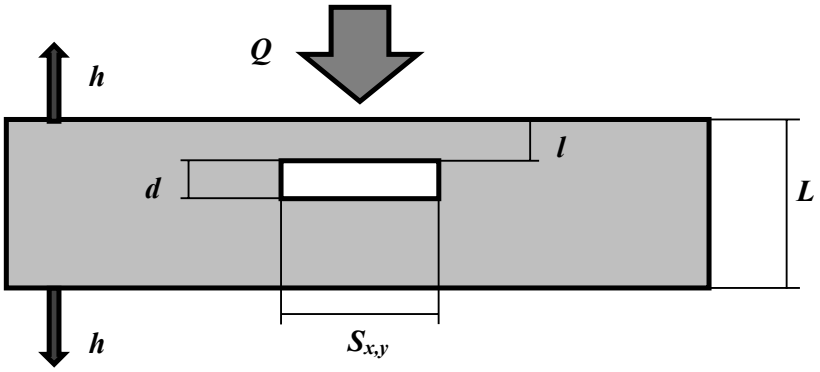

Figure 1. Basic TNDT scheme

If to assume that the present of subsurface discontinuities in a material causes a change in its local or integral thermal properties, the scheme of Fig. 1 can be used for both defect detection and thermal property measurement that is an important issue in high-tech industries, particularly, aerospace.

The front-surface temperature described by Eq. (1) decreases monotonically from a maximum value to the ambient temperature and reveals no characteristic points which can be used for determining diffusivity. However, some approaches have been developed to determining material diffusivity in a one-sided test of which probably the most feasible are those involving non-linear fitting [2, 3]. In [4] and recently in [5], it was suggested to analyze a pixel-based artificial function obtained by multiplying a front-surface temperature evolution by the time to power n ($T \times Fo^n$), where n=0.1-1. Below we call this approach 'time-to power n'.

Figure 2 shows the family of curves $T \times Fo^n$ *vs.* Fo. In fact, as shown in [4], in order to provide clear minimums $\tau_{\min}$ in the artificial function, one should use n from 0.1 to 0.5 when determining diffusivity in the case of Dirac-pulse adiabatic heating. In this paper, we extend this approach on non-adiabatic samples heated with a τ_h - long heat pulse.

The relationship between the minimum time $Fo_{\min}$ and n was found in the following form [5]:

$$Fo_{\min} = 0.627206 - 2.21971\,n + 5.41918\,n^2 - 5.96047\,n^3 . \quad (2)$$

An optimal n should provide the steepest derivative of the $T(\tau) \times \tau^n$ near a minimum point, and it is n=0.41 ($Fo_{\min}$=0.2169) if one deals with Dirac-pulse diffusivity measurement [5]. For n=0.41, material diffusivity can be found by the formula similar to Parker's one:

$$a = 0.2169 L^2 / \tau_{\min} . \quad (3)$$

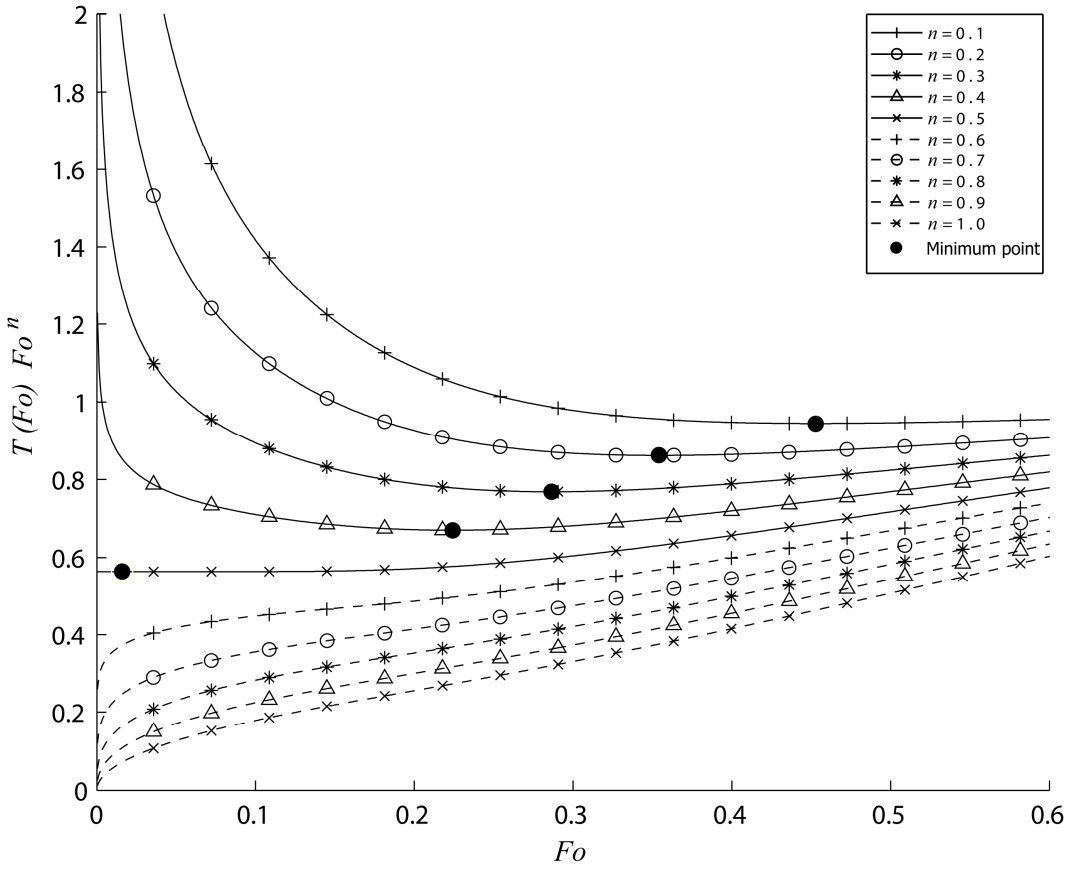

Figure 2. Artificial function $T \times Fo^n$ *vs.* Fo for n=0.1 -1.0 and minimums for n=0.1-0.5 ([5])

3. DETERMINING THERMAL DIFFUSIVITY (ARTIFICIAL IMAGE SEQUENCE)

Two artificial sequences consisted of 150 images were calculated for the front and rear surfaces of a 2 mm-thick glass fiber reinforced plastic (GFRP: conductivity 0.38 $Wm^{-1}K^{-1}$, diffusivity $1.7 \cdot 10^{-7}$ m^2s^{-1}, heat exchange coefficient on both surface 10 $Wm^{-2}K^{-1}$) sample heated with a heat pulse (τ_h=0.1 s, calculation step 0.1 s) through an experimental spatial mask. One of front-surface experimental images of a defect-free GFRP sample heated with 6×5 kW halogen lamps was chosen as the mask.

The known two-sided Parker's technique was chosen as a reference in diffusivity measurement. Figure 3a shows the temperature distribution on the rear surface of the defect-free GFRP sample at the time 3.3 s that is approximately the time $\tau_{1/2}$ when the rear surface temperature reaches a half of its maximum value. This distribution reflects the mask used for making heating uneven across the heated surface. The diffusivity map calculated by Parker's formula $a = 0.139L^2 / \tau_{1/2}$ is shown in Fig. 3b. The mean diffusivity value in this map is $1.81 \cdot 10^{-7}$ m^2s^{-1}. The deviation from the true value used in the calculation can be explained by the presence of surface heat exchange and the finite heat pulse duration. However, it is worth noting the very uniform character of the diffusivity map which is independent of the uneven heating pattern.

Front-surface test results are presented in Fig. 3c-e. The temperature distribution in Fig. 3c repeats the one on the rear surface because of the mask used. The timegram in Fig. 3d was obtained by the minimum of the function $T(\tau)\times\tau^{0.41}$ which occurred at 4.2 s (the mean value across the sample) as shown in Fig. 3e. Note that the very first curve minimum in Fig. 3e which occurred in the first image was discarded because it was conditioned by the finite duration of the heat pulse. The corresponding diffusivity value was calculated by Eq. (3): $a = 2.1\cdot10^{-7}$ m^{2}s^{-1}.

This value is about 20 % greater than the true one and 10% greater than that calculated by the rear surface. Again, this can be explained by the fact that the front surface is more prone to surface heat exchange than the rear surface. However, we consider the proposed technique as probably more convenient for reference-free front-surface defect detection rather than for accurate measurement of diffusivity.

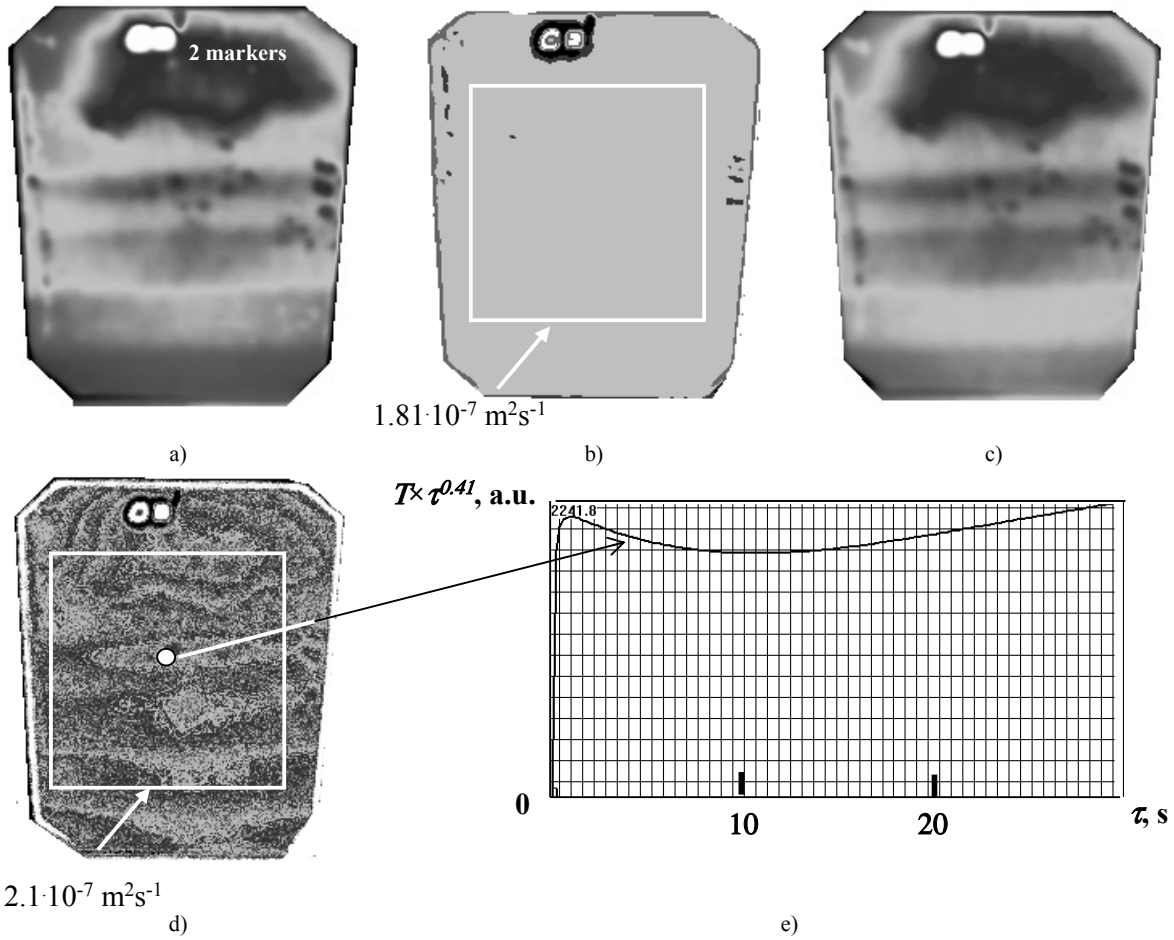

Figure 3. Determining thermal diffusivity of 2 mm-thick GFRP sample heated through spatial mask (pulse duration 0.1 s):

a – rear-surface temperature distribution at 3.3 s,
b – rear-surface map of diffusivity,
c – front-surface temperature distribution at 4.32 s,
d – front-surface map of diffusivity,
e – $T(\tau)\times\tau^{0.41}$ *vs.* τ

4. APPLYING THE TIME-TO POWER *n* APPROACH TO DEFECT DETECTION (ARTIFICIAL IMAGE SEQUENCE)

In order to compare theoretical and experimental results in a more realistic way, the front-surface artificial image sequence was calculated for a 6 mm-thick GFRP sample having 9 defects similar to those introduced in the experimental reference sample described below (Fig. 4a). The sequence contained 200 images taken with the time interval of 0.25 s (see the example in Fig. 4b). By trial, it was found that optimum detection conditions occurred if n~0.57. Note that, unlike the results discussed in Sections 2 and 3, in this case the heating was relatively long (5 s) and the sample was non-adiabatic, therefore, the conclusion on the optimum value n=0.41 seems to be no more valid for long heating of defective materials. For n=0.57, the defect areas revealed the minimums which were quite clear for shallow defects and rather flat for deeper ones (Fig. 4c). The timegram in Fig. 4d distinctly shows all modeled defects while lower values of n lead to 'disappearance' of small/deep defects. Another feature of the front-surface timegram in Fig. 4d is the suppressed pattern of uneven heating and good separation of defects by $\tau_{\min}$, i.e. by defect depth l. This can be used to produce thermal tomograms shown in Fig. 4e, f in the same way as by using the earlier-proposed algorithm of dynamic thermal tomography where choosing a reference point is the feature typically criticized [4]. Square shape of all defects at the depth of 2 mm is clearly seen while the image of the deeper (l=4 mm) defects is accompanied with artifacts which represent 'footprints' of shallower defects (see defect contours in Fig. 4f).

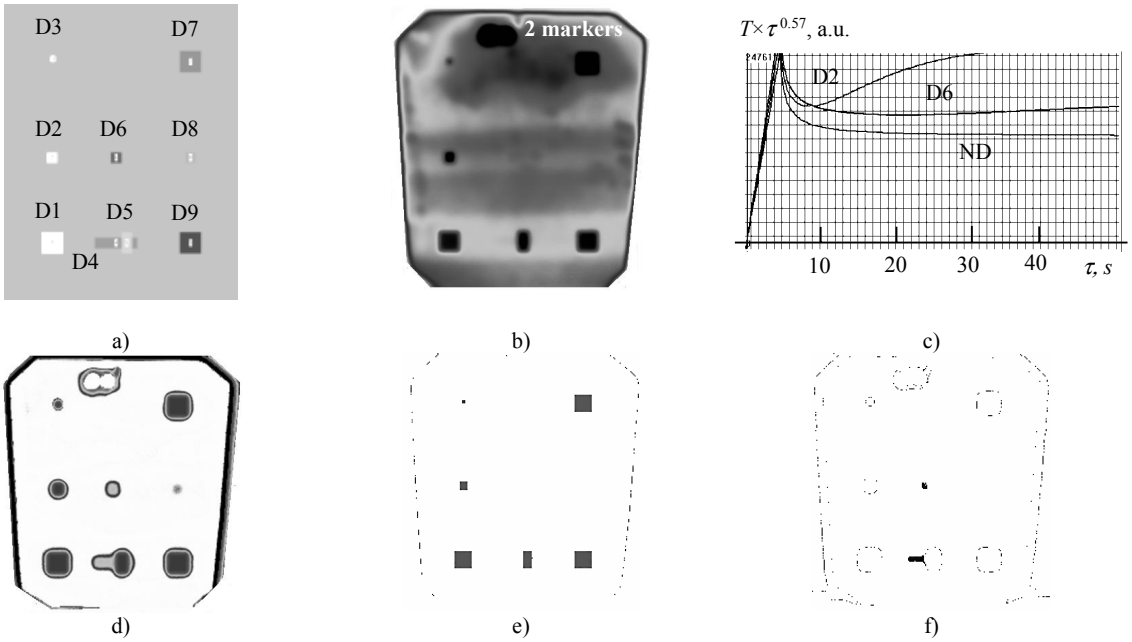

Figure 4. Applying the time-to power n approach to processing of an artificial sequence (heating the 10 mm-thick GFRP sample with defects for 5 s):

a – defect scheme (D1: 20x20x2, l=2 mm; D2: 10x10x2, l=2 mm; D3: 5x5x2, l=2 mm; D4: 40x10x2, l=4 mm; D5: 10x20x2, l=2 mm; D6: 10x10x2, l=4 mm; D7: 20x20x2, l=2 mm; D8: 10x10x2, l=6 mm; D9: 20x20x2, l=2 mm,
b – example of calculated IR thermogram,
c – $T(\tau)\times\tau^{0.57}$ *vs.* τ,
d – timegram (n=0.57),
e – tomogram (n=0.57, τ=5-7.5 s),
f – tomogram (n=0.57, τ=16-17.5 s)

5. APPLYING THE TIME-TO POWER *n* APPROACH TO DEFECT DETECTION (EXPERIMENTAL IMAGE SEQUENCE)

A reference sample was manufactured according to the scheme in Fig. 4a. The sample included 5 GFRP plates of the 2 mm thickness each glued together with epoxy adhesive. The defects were produced as cuts in particular plates thus having thickness 2 mm. Five tubular halogen lamps with the total power of 5x6 kW were used for heating the sample for 5 s. Both the heating and cooling stages were recorded with the frame frequency of 10 Hz but only the cooling stage was used for calculating $T \times \tau^n$ pixel functions. Source images, such as in Fig. 5a, reveal the uneven strip-like heating pattern caused by tubular lamps (we remind that this pattern was used as the spatial mask in modeling, see images in Fig. 3 and 4). The Fourier phasegram is presented in Fig. 5b as a reference because it is often believed that the use of the Fourier transform ensures efficient suppression of uneven heating phenomena. In fact, the image in Fig. 5b looks rather uniform even if the defects D6 and D8 are not seen.

Again, when analyzing minimums of the experimental curves, the optimum value of n~0.62 was found by trial. The $T(\tau)\times\tau^{0.62}$ curves which are shown in Fig. 5c for the defects D1, D2 and a non-defect area look similar to the theoretical profiles in Fig. 4c. The corresponding timegram in Fig. 5d shows all modeled defects except the D8 which is located at the depth of 6 mm. The example of the thermal tomogram is presented in Fig. 5e for the layer from 2 to 4 mm.

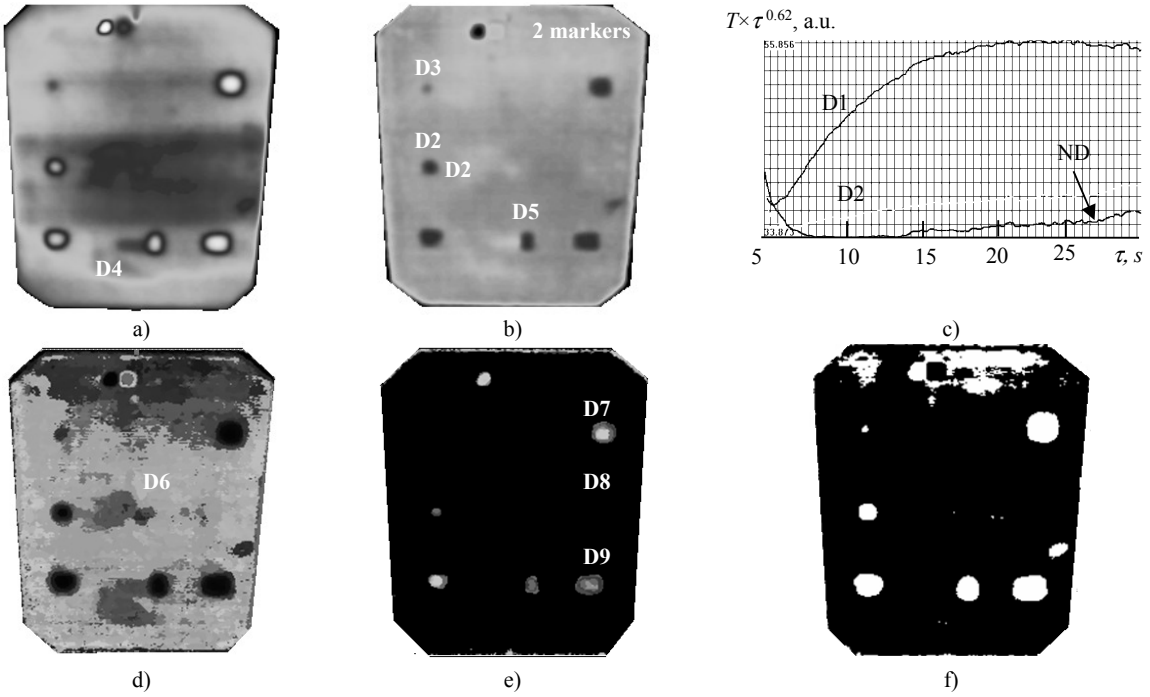

Figure 5. Processing results by the time-to power *n* algorithm (model from Fig. 4a):

a – optimum source image,
b - Fourier phasegram,
c – $T(\tau)\times\tau^{0.62}$ *vs.* τ,
d– timegram by minimum (n=0.62),
e– tomogram by minimum (n=0.62, time interval 5.2-7.2 s),
f – tomogram by maximum (n=0.62, time interval 7-9 s)

Another finding in the analysis of experimental data was the presence of local maximums in $T(\tau)\times\tau^n$ curves that can be also used for defect separation by layers. This case is illustrated in Fig. 5f for n=0.62.

6. CONCLUSION

The approach discussed in this study introduces one more technique of front-surface data processing in TNDT. By producing pixel-based $T(\tau)\times\tau^n$ functions it is possible to artificially create characteristic points, such as local maximums and minimums, of which observation time is related to thermal diffusivity and defect depth. In the case of defect-free materials, this technique can be used for evaluating material thermal diffusivity by the formulas analogous to the classical Parker expression. When applied to defective samples, the thermal tomography technique can be implemented to synthesize timegrams which, in their turn, can be sliced for thermal tomograms.

This research was supported in part by NIR # 445 (ONG), State order of the Russian Ministry of Higher Education for 2014-2016, and by the grant # 8.1.27.2015 from "The Tomsk State University Academic D.I. Mendeleev Fund Program".

REFERENCES

[1] Parker, W.J., Jenkins, R.J., C. Butter, C.P. and Abbott, G.L., "Flash method of determining thermal diffusivity, heat capacity and thermal conductivity", J. Appl. Phys. 32, 1679-1689 (1961).
[2] Grinzato, E. and Marinetti, S., "Materials NDE by non-linear filtering applying heat transfer models", Advances in signal processing for non destructive evaluation of materials, ed. by X. Maldague, NATO ASI Series, Series E: Applied Sciences, Kluwer Academic Publishers 262, 117-132 (1994).
[3] Zalameda, J.N. and Winfree, W.P., "Improved sampling of thermal transients using Focal Plane Array infrared imagers", Proc. SPIE 5405, 374-381 (2004).
[4] Vavilov, V.P., "Dynamic thermal tomography: Recent improvements and applications", NDT & E International 71, 23-32 (2015).
[5] Vavilov, V.P. and Pawar, S., "A novel approach for one-sided thermal nondestructive testing of composites by using infrared thermography", Polym. Test., (submitted paper).